

# Signatures of Incomplete Paschen-Back Splitting in the Polarization Profiles of the He I 10830 Å multiplet

H. Socas-Navarro

*High Altitude Observatory, NCAR<sup>1</sup>, 3450 Mitchell Lane, Boulder, CO 80307-3000, USA*  
 navarro@ucar.edu

J. Trujillo Bueno <sup>2</sup>

*Instituto de Astrofísica de Canarias, Avda Vía Láctea S/N, La Laguna 38205, Tenerife, Spain*  
 jtb@iac.es

E. Landi Degl'Innocenti

*Dipartimento di Astronomia e Scienza dello Spazio, Largo E. Fermi 2, 50125 Firenze, Italy*  
 landie@arcetri.astro.it

## ABSTRACT

We investigate the formation of polarization profiles induced by a magnetic field in the He I multiplet at 10830 Å. Our analysis considers the Zeeman splitting in the incomplete Paschen-Back regime. The effects turn out to be important and produce measurable signatures on the profiles, even for fields significantly weaker than the level-crossing field ( $\sim 400$  G). When compared to profiles calculated with the usual linear Zeeman effect, the incomplete Paschen-Back profiles exhibit the following conspicuous differences: a) a non-Doppler blueshift of the Stokes V zero-crossing wavelength of the blue component; b) area and peak asymmetries, even in the absence of velocity and magnetic gradients; c) a  $\sim 25\%$  reduction in the amplitude of the red component. These features do not vanish in the weak field limit. The spectral signatures that we analyze in this paper may be found in previous observations published in the literature.

*Subject headings:* line: profiles – Sun: atmosphere – Sun: magnetic fields – Sun: chromosphere

## 1. Introduction

Many of the physical challenges of solar and stellar physics arise from magnetic processes taking place in the outer regions of the atmosphere. Unfortunately, our present empirical knowledge on the magnetism of the chromosphere, transition region and corona is still very crude. In our opinion, there are two key avenues that should be pursued to improve the situation.

Firstly, new instrumentation is needed, including a space-borne UV polarimeter and a large ground-based solar telescope optimized for (spectro-)polarimetric observations (e.g., the Advanced Technology Solar Telescope). Secondly, but equally importantly, we need appropriate diagnostic tools that will permit us to infer the magnetic field vector from the observed polarization in suitably chosen spectral (chromospheric and coronal) lines. The present paper represents a contribution to this second line of research.

In particular, our aim here is to demonstrate that the determination of the magnetic field vector via the analysis of the observed polarization in the He I 10830 Å multiplet must be carried out considering the wavelength positions and the strengths of the Zeeman components in the incomplete Paschen-Back effect regime. Previous research done with this multiplet has ignored this effect (with the only exception of Trujillo Bueno et al. 2002), which re-

sulted in considerable confusion surrounding the formation physics of these lines.

The He I 10830 Å multiplet originates between a lower term ( $2^3S_1$ ) and an upper term ( $2^3P_{2,1,0}$ ). Therefore, it comprises three spectral lines (see, e.g., Radzig & Smirnov 1985): a ‘blue’ component at 10829.09 Å with  $J_l = 1$  and  $J_u = 0$  (hereafter Transition 1, or Tr1 for abbreviation), and two ‘red’ components at 10830.25 Å with  $J_u = 1$  (hereafter, Tr2) and at 10830.34 Å with  $J_u = 2$  (hereafter, Tr3) which appear blended at solar atmospheric temperatures. As shown in Fig 1, the energy difference between the levels with  $J_u = 2$  and  $J_u = 1$  is such that their respective magnetic substates cross each other for magnetic strengths between 400 G and 1500 G, approximately. Therefore, *at least* in this range of strengths, the Zeeman splitting of such  $J$ -levels is comparable to their energy separation. As a result, the perturbation theory of the familiar Zeeman effect is no longer valid. The energy positions of the magnetic substates as a function of the field strength have to be calculated in the incomplete Paschen-Back effect regime, which requires to diagonalize the *total* Hamiltonian (see, e.g., Condon & Shortley 1970). Interestingly, as we shall see below, the proper calculation of the Zeeman components results in significant differences in the Stokes profiles that emerge from a magnetized stellar atmosphere. Furthermore, such differences do not vanish in the limit of weak fields.

The outline of this paper is as follows. Section 2 presents a brief review of the Paschen-Back effect theory, illustrating the range of magnetic strengths for which the  $J$ -levels of the  $2^3P_{2,1,0}$  term cross. Section

---

<sup>1</sup>The National Center for Atmospheric Research (NCAR) is sponsored by the National Science Foundation.

<sup>2</sup>Consejo Superior de Investigaciones Científicas, Spain

3 shows a detailed comparison of the results that we have obtained assuming linear Zeeman splitting (LZS) or incomplete Paschen-Back splittings (IPBS), including an analytical demonstration that explains our numerical radiative transfer results in a Milne-Eddington model. Finally, Section 4 gives our concluding remarks.

## 2. The Paschen-Back effect

According to the theory of the Zeeman effect (see, e.g., Condon & Shortley 1970) the corrections to the degenerate energy  $E_J$  of any atomic level of total angular momentum quantum number  $J$  are obtained by diagonalizing the matrix  $\langle JM|H_B|JM' \rangle$ , where  $H_B$  is the magnetic Hamiltonian, given by:

$$H_B = \mu_0(\vec{L} + 2\vec{S})\vec{B}, \quad (1)$$

with  $\mu_0 = 9.27 \times 10^{-21}$  erg G<sup>-1</sup> being the Bohr magneton. By choosing the quantization z-axis of total angular momentum along the magnetic field vector, one finds:

$$\langle JM|H_B|JM' \rangle = \mu_0 B g M \delta_{MM'} \quad (2)$$

where  $g$  is the Landé factor. This equation shows that, to first order of perturbation theory, any atomic level of total angular momentum quantum number  $J$  is split by the action of a magnetic field into  $(2J + 1)$  *equally spaced* sublevels, the splitting being proportional to the Landé factor  $g$  and to the magnetic field strength. It is important to note that a state of the form  $|JM \rangle$  is an eigenvector of the *total* Hamiltonian ( $H_0 + H_B$ ), with eigenvalue  $E_J + \mu_0 B g M$ , only when the z-axis of the reference system points in the direction of the magnetic field.

The previous well-known results of first-order perturbation theory are correct only if the splitting produced by the magnetic field on a  $J$ -level is small compared to the energy separation between the different  $J$ -levels of the  $(L, S)$  term under consideration. In other words, the standard theory of the Zeeman effect is valid only in the limit of “weak” magnetic fields. Here, “weak” means that the coupling of either the spin or the orbital angular momentum to the magnetic field is *weaker* than the coupling between the spin and the orbital angular momentum (the spin-orbit coupling). This is the so-called *Zeeman effect regime*.

In the opposite limit, the magnetic field is so “strong” that the spin-orbit interaction can be considered as a perturbation compared to the magnetic interaction. In this case the magnetic field dissolves the fine structure coupling – that is,  $\vec{L}$  and  $\vec{S}$  are practically decoupled and precess independently around  $\vec{B}$ . Therefore, the quantum number  $J$  loses its meaning. In this so-called *complete Paschen-Back effect regime* the magnetic Hamiltonian is diagonal on the basis  $|LSM_L M_S \rangle$ , and the eigenvalues are given by:

$$\langle LSM_L M_S|H_B|LSM_L M_S \rangle = \mu_0 B (M_L + 2M_S). \quad (3)$$

In this “strong” field regime, the term  $(L, S)$  splits into a number of components, each of which corresponds to particular values of  $(M_L + 2M_S)$ . In the presence of a magnetic field, the corrections to the energy of the state  $|LSM_L M_S \rangle$  due to the spin-orbit interaction has the form  $\langle A\vec{L} \cdot \vec{S} \rangle = A M_L M_S$ , where  $A$  is a constant with dimensions of energy.

It is of interest to note that, since the

spin-orbit coupling increases rapidly with increasing nuclear charge, the conditions for a “strong” field are met at a much lower field with light atoms (like helium) than with heavy atoms. In fact, as shown in Fig 1, the levels with  $J = 2$  and  $J = 1$  of the upper term  $^3P$  of the He I 10830 Å multiplet cross for magnetic strengths between 400 G and 1500 G, approximately. This level-crossing regime corresponds to the *incomplete Paschen-Back effect regime*, in which the energy eigenvectors are gradually evolving from the form  $|LSJM\rangle$  to the form  $|LSM_L M_S\rangle$  as the magnetic field increases. This range between the limiting cases of “weak” fields (Zeeman effect regime) and “strong” fields (complete Paschen-Back regime) is more difficult to analyze since it implies the evaluation of matrix elements of the form  $\langle JM|H_B|J'M'\rangle$ , which (in general) can only be done numerically. To this aim, we have developed a numerical code capable of computing, for a magnetic field of arbitrary intensity, the strengths and the splittings of the  $\sigma$  and  $\pi$  components in a line multiplet arising from the transition between two ( $L, S$ ) terms. This code is very similar to a previous one that solves the problem of the intermediate Paschen-Back effect in a line with hyperfine structure (Landi Degl’Innocenti 1978).

### 3. Results

We have developed a numerical code for the synthesis and inversion of Stokes profiles in a Milne-Eddington atmosphere, considering IPBS as described in §2. This code has been built with the aim of analyzing spectropolarimetric observations of solar active regions, but we shall use it here

to explore the effects of IPBS on the 10830 polarization profiles.

We consider a reference model atmosphere and calculate the multiplet component positions and strengths for various magnetic fields (ranging from 0 to 3 kG). The Zeeman components are calculated accounting for IPBS and then compared to the usual approximation of LZS. The most relevant parameters of the chosen Milne-Eddington model are  $\eta_0 = 4$ ,  $\Delta\lambda_D = 105$  mÅ,  $B_0 = 0.8$ ,  $B_1 = 0.2$ ,  $a = 0.8$  (see, e.g., Landi Degl’Innocenti 1992 for definitions of the Milne-Eddington parameters). Sample profiles are depicted in Fig 2 for a 500 G field with an inclination of  $50^\circ$  from the line of sight. There are a few obvious differences between the IPBS and LZS Stokes V profiles: a) The blue component of the multiplet, Tr1, shows a net asymmetry with a global offset towards negative values;<sup>3</sup> b) A small non-Doppler blueshift of the same component (which is actually related to the asymmetry); c) A reduced amplitude of the red and blue lobes of the red component of the multiplet (Tr2 and Tr3). The linear polarization profiles exhibit also some small asymmetry. These differences are due to IPBS effects on the Zeeman components of the transitions, discussed in §3.1 below.

In order to compare the IPB results with the LZS ones, one needs the relative strengths and effective Landé factors of the three components. These are listed in Table 1. Note that some of the values do not coincide with those used by

---

<sup>3</sup>The sign of this offset depends on the polarity of the profile. It is produced by an imbalance in the weights of the  $\sigma$  components of this transition, with the red component being stronger.

TABLE 1  
 ATOMIC PARAMETERS USED IN THE CALCULATIONS

$\lambda$ (Å)	Lower term	Upper term	$g_{eff}$	Relative strength
10829.09	$^3S_1$	$^3P_0$	2.00	0.111
10830.25	$^3S_1$	$^3P_1$	1.75	0.333
10830.34	$^3S_1$	$^3P_2$	1.25	0.556

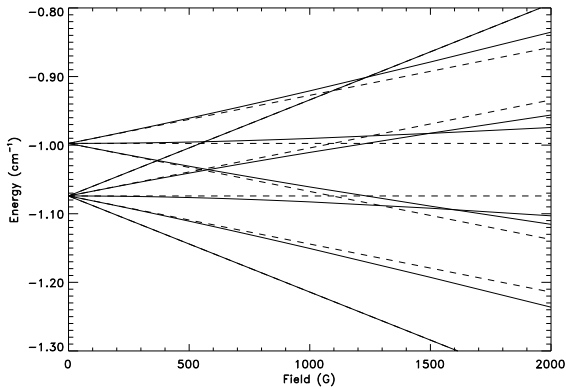


Fig. 1.— Energy diagram for the upper levels of Tr2 and Tr3 (the  $^3P_1$  and  $^3P_2$  levels of the multiplet). Solid: IPBS. Dashed: LZS. Note the numerous level crossings between 400 and 1500 G, approximately. Energies are in  $\text{cm}^{-1}$  with respect to the  $J=0$  level.

other authors in previous works. For example, concerning the LZS calculations the effective Landé factor ( $g_{eff}$ ) of Tr3 is 1.25, whereas Rüedi et al. (1995) and Lagg et al. (2004) take it to be 0.875. The relative strengths<sup>4</sup> ( $f_i$ ) of Tr1, Tr2 and Tr3 are here 0.111, 0.333 and 0.556, respectively. Our  $f_i$  agree with those of Rüedi et al. (1995), but not with Lagg et al. (2004) (these authors quote *relative oscillator strengths*, but the conversion is straightforward). It is not completely clear to us what the source of the discrepancy is. For the  $g_{eff}$  we used its standard definition (e.g., Landi Degl’Innocenti 1992) applied to the quantum numbers shown in the table. The  $f_i$  are calculated according to the usual formulae (e.g., Radzig & Smirnov 1985). Thus, both of these quantities are derived straightforwardly from well-known atomic parameters. As we discuss below, it is not possible to reproduce the observations using the LZS approximation. It is conceivable that other authors had to modify their atomic parameters in an attempt to compensate for IPBS effects. This would allow

<sup>4</sup>Note that the symbol  $f_i$ , which is used here and in other previous works on this multiplet, refers to the relative strengths of the components. These are not the “oscillator strengths” of the transitions, which are also commonly denoted by  $f_i$ .

them to fit observed profiles with those calculated using LZS. For example, the ratio of Stokes V amplitudes of the blue and red components calculated with LZS is significantly larger than it should be. Artificially reducing the  $g_{eff}$  of Tr3 reduces the amplitude of the red component without affecting the intensity profiles, thus bringing the profiles closer to the observations.

### 3.1. Zeeman components

The positions (with respect to the zero-field wavelength) and strengths of the various  $\pi$  and  $\sigma$  components of the multiplet are shown in Fig 3. Tables 2 to 4 list the actual IPBS values at 500 G, which are also useful to match the curves in the left and right panels. Note that the positions of the Tr1 components are not significantly disturbed by the presence of the other levels ( $J=1$  and  $J=2$ ) in the field range depicted in the plots. However, the strength of the  $\sigma$  components is indeed perturbed, introducing an asymmetry between the left- and right-handed polarizations. For our discussions in §3.2 below it is important to note that this asymmetry increases linearly with the magnetic field.

The positions of the Tr2 and Tr3 components feel a much stronger perturbation for fields stronger than  $\sim 500$  G. This is due to the close proximity in the energy diagram of the upper levels of these transitions (the  $J = 1$  and  $J = 2$  levels). Similarly to the case of Tr1, the component strengths of Tr2 and Tr3 become asymmetric. The asymmetry is rather linear for weak fields. As the field increases above  $\sim 500$  G, however, the behavior of the component strengths becomes non-linear.

Finally, it is interesting to note the pres-

ence of a  $\pi$  component in Tr2 that does not exist in the LZS approximation. This new component appears for non-zero fields in IPBS and becomes more important as the field increases.

The asymmetries between left- and right-handed  $\sigma$  components in all three transitions, are important. They ultimately manifest themselves as asymmetries in the profiles and lead to net circular polarization even in the absence of velocity or magnetic field gradients.

### 3.2. Weak-field asymptotic behavior

Fig 3 shows that the Zeeman components of the various transitions tend towards the LZS values as the magnetic strength goes to zero. One may thus expect that the IPBS profiles (plotted in the top row) would become similar to the LZS profiles in the weak field limit. However, this is not the case. The profiles obtained from our calculations maintain their shape unchanged down to the lower limit of our simulation (0.1 G). This apparent paradox has a simple, albeit slightly counterintuitive, explanation. The Stokes V profiles can be described conceptually as the subtraction of two bell-type functions, similar to Gaussians or Lorentzians. In the weak field limit the separation between these functions is much smaller than their width, and the resulting Stokes V profile is essentially a small residual of the subtraction. A slight asymmetry between the two functions will show more conspicuously the closer together they are. Therefore, reducing the field results in “amplifying” the red/blue asymmetries. Let us analyze this in some detail considering a very simple

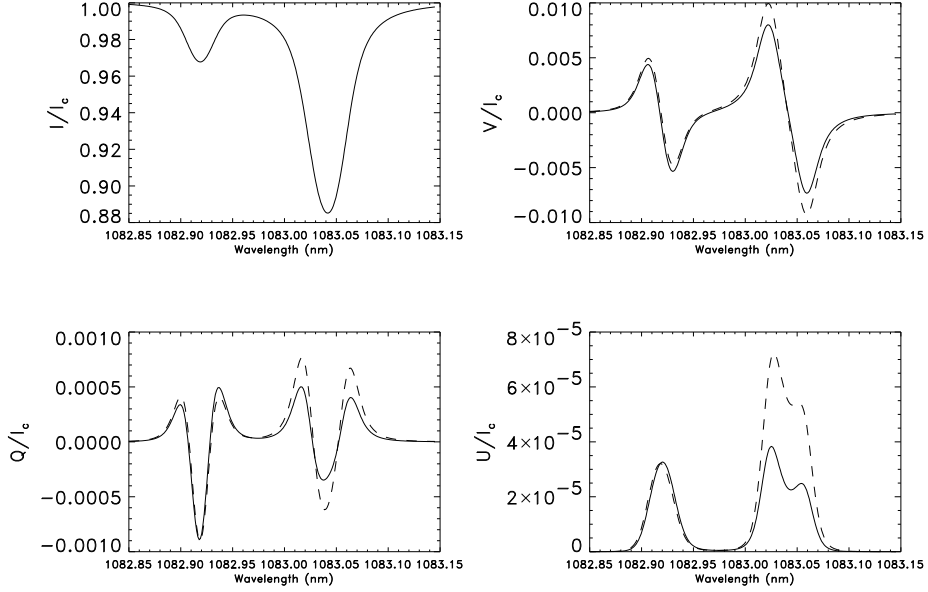


Fig. 2.— Simulated Stokes profiles of the 10830 Å multiplet, assuming a 500 G field inclined 50° with respect to the line of sight. The profiles are normalized to the quiet sun continuum intensity ( $I_c$ ).

TABLE 2  
COMPONENT POSITIONS AND STRENGTHS FOR TR1 (500 G)

Type of component	Position (Doppler units)	Strength
$\sigma^+$	0.524	0.106
$\pi$	0.004	0.111
$\sigma^-$	-0.516	0.116

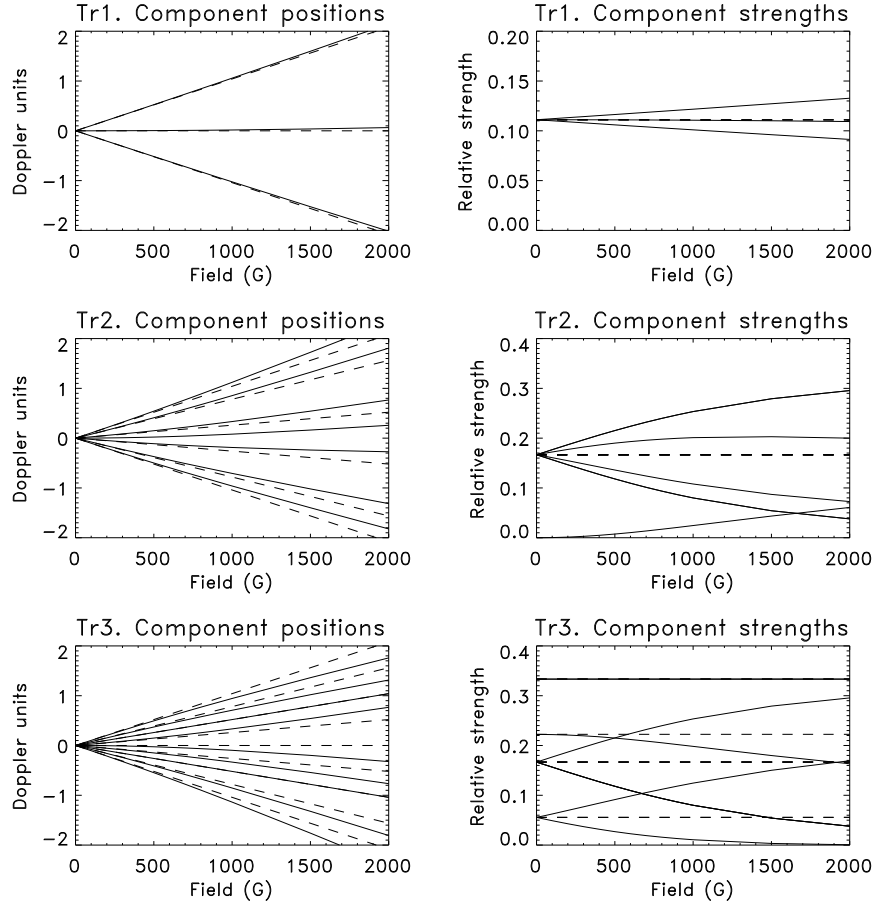


Fig. 3.— Positions and strengths of the Zeeman components as a function of the magnetic field. In all panels the solid lines represent calculations considering IPBS while the dashed lines represent those using the LZS approximation. Note that, in the general IPBS case, the Zeeman components exhibit asymmetric displacements and strengths. Also notice that the Zeeman IPBS components have strengths that depend on the magnetic field.



TABLE 3  
 COMPONENT POSITIONS AND STRENGTHS FOR TR2 (500 G)

Type of component	Position (Doppler units)	Strength
$\sigma^+$	0.542	0.136
$\sigma^+$	0.410	0.118
$\pi$	0.149	0.118
$\pi$	0.022	0.007
$\pi$	-0.111	0.215
$\sigma^-$	-0.371	0.215
$\sigma^-$	-0.499	0.190

TABLE 4  
 COMPONENT POSITIONS AND STRENGTHS FOR TR3 (500 G)

Type of component	Position (Doppler units)	Strength
$\sigma^+$	0.495	0.091
$\sigma^+$	0.371	0.215
$\sigma^+$	0.260	0.333
$\pi$	0.111	0.215
$\pi$	-0.025	0.215
$\pi$	-0.149	0.118
$\sigma^-$	-0.260	0.333
$\sigma^-$	-0.410	0.118
$\sigma^-$	-0.546	0.027

scenario. Suppose that we have a Stokes V profile that is the result of subtracting two Gaussians separated by a small distance  $2\Delta x$ :

$$V(x) = Ae^{-(x-\Delta x)^2} - Be^{-(x+\Delta x)^2}. \quad (4)$$

The zero-crossing wavelength ( $x_0$ ) of  $V(x)$  is given by the condition:

$$Ae^{-(x_0-\Delta x)^2} = Be^{-(x_0+\Delta x)^2}, \quad (5)$$

which, taking logarithms on both sides, leads to:

$$x_0 = \frac{\log(B/A)}{4\Delta x}. \quad (6)$$

If the asymmetry is small ( $B/A \simeq 1$ ), a Taylor expansion of the logarithm yields:

$$x_0 \simeq \frac{B-A}{4B\Delta x}. \quad (7)$$

For weak fields, the asymmetry  $B-A$  depends linearly on the field ( $\Delta x$ ). We then conclude that:

$$x_0 \propto \frac{1}{4B}, \quad (8)$$

i.e., the zero-crossing wavelength is shifted and does *not* depend on the magnetic field. In the derivation above we have been concerned only with strength asymmetries, neglecting the effect of asymmetric component positions. If we denote by  $\Delta x_A$  and  $\Delta x_B$  the (different) component positions, a similar straightforward reasoning can be conducted to conclude that:

$$x_0 \simeq \frac{B-A}{4B\overline{\Delta x}} + \frac{1}{2}(\Delta x_A - \Delta x_B), \quad (9)$$

where  $\overline{\Delta x} = (\Delta x_A + \Delta x_B)/2$ . It is evident from Eq (9) that position asymmetries have only a second-order effect on  $x_0$ , since  $(\Delta x_A - \Delta x_B)$  is proportional to  $\overline{\Delta x}$ .

We verified this property with our simulations.

Consider now the area asymmetry:

$$\mathcal{A} = \frac{\int_{-\infty}^{\infty} V(x)dx}{\int_{-\infty}^{\infty} |V(x)|dx}. \quad (10)$$

In the weak-field limit, the denominator of Eq (10) is directly proportional to the field. Thus:

$$\mathcal{A} \simeq \frac{c}{\Delta x} \int_{-\infty}^{\infty} V(x)dx, \quad (11)$$

where  $c$  is a constant. Expanding the exponentials in Eq (4) in a Taylor series and truncating to first order, we obtain that for  $\Delta x \ll 1$ :

$$e^{-(x-\Delta x)^2} \simeq e^{-x^2} + 2xe^{-x^2}\Delta x. \quad (12)$$

Thus:

$$V(x) \simeq (A-B)e^{-x^2} + 2xe^{-x^2}\Delta x(A+B). \quad (13)$$

Inserting this into Eq (11) and taking into account the odd parity of the second term in Eq (13), it is evident that:

$$\mathcal{A} \simeq c\sqrt{\pi}\frac{A-B}{\Delta x}. \quad (14)$$

Therefore, the net area asymmetry  $\mathcal{A}$  remains constant even for fields approaching zero. All of the asymptotic properties of Stokes V derived in this section (constancy of the zero-crossing wavelength, net asymmetry, relative importance of weight and position asymmetries) have been confirmed by further modeling using our numerical code. It is important to note that the results we present here do not violate the principle of spectroscopic stability, since the Zeeman components (and their

center of gravity) approach asymptotically the LZS values.

The asymptotic values that we obtained for Tr1 are  $x_0=340 \text{ m s}^{-1}$  and  $|\mathcal{A}|=0.11$  (with the red lobe having a larger area). It must be noted that this value of  $\mathcal{A}$  is influenced by the blend with the blue wing of the red component. We estimated the effect of this blend by calculating  $\mathcal{A}$  for the LZS profile (which should be zero), obtaining  $|\mathcal{A}_{LZS}|=0.04$ . In this case it is the blue lobe that has larger area. Therefore, the presence of the blend has the effect of reducing the  $|\mathcal{A}|$  of the IPBS profile. The actual value of  $x_0$  is significantly model-dependent. In particular, it is very sensitive to the Doppler width of the line. Doubling this parameter in our model, resulted in a factor 4 increase of  $x_0$ . For the red component of the multiplet (Tr2 and Tr3), we obtained  $x_0=95 \text{ m s}^{-1}$  and  $|\mathcal{A}|=0.05$ . Here, as opposed to Tr1, the zero-crossing is redshifted and the blue lobe has a larger area. The dependence of  $x_0$  and  $|\mathcal{A}|$  for both lines are plotted in Figs 4 and 5.

#### 4. Conclusions

The calculations reported in this paper show that IPBS effects need to be taken into account for proper diagnostics based on the He I multiplet at  $10830 \text{ \AA}$ . This is a very interesting set of lines, with some unique properties that make it an ideal tool for the exploration of chromospheric and coronal magnetism. Care must be taken, however, to consider all the relevant physical processes that intervene in the formation of the lines.

The (still few) works existing in the literature regarding Stokes observations of these lines do not seem to agree on

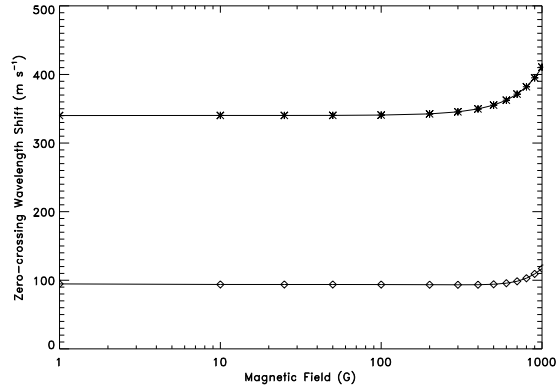


Fig. 4.— Relative Stokes V zero-crossing shift between IPBS and LZS profiles (absolute value), as a function of the field strength. Stars: blue component (Tr1). Diamonds: red component (Tr2+Tr3). The Tr1 shift is towards the blue, whereas the Tr2+Tr3 shift is towards the red.

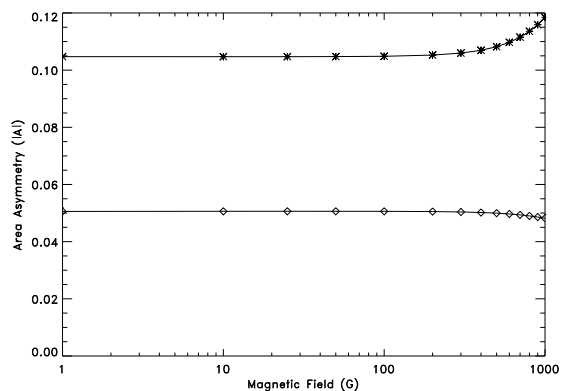


Fig. 5.— Area asymmetry ( $|\mathcal{A}|$ ) of the IPBS profiles as a function of the field strength. Stars: blue component (Tr1). Diamonds: red component (Tr2+Tr3). Tr1 has a larger red lobe, whereas Tr2+Tr3 has a larger blue lobe.

such fundamental parameters as: the rest wavelength of the Tr1 line; the effective Landé factor of the Tr3 line; the relative strengths of the transitions (compare the values given in Rüedi et al. 1995; Lagg et al. 2004; this work). These are basic parameters that should be well known, either from laboratory experiments or from very simple calculations. We believe that, at least partly, the existing confusion might have its origin in neglecting IPBS effects. We have shown that IPBS is responsible for a non-Doppler blueshift of Tr1, systematic profile asymmetries and a reduced amplitude of Stokes V in the Tr2+Tr3 blend. As an illustrative example, consider the simple line-ratio experiment represented in Fig 6. For a fixed model atmosphere, the ratio of Stokes V amplitudes in the red (Tr2+Tr3) and the blue (Tr1) components of the multiplet depends smoothly on the magnetic field. It is clear from the figure that neglecting IPBS leads to an erroneous estimate of the field. Interestingly, the IPBS curve is steeper than the LZS one, indicating that it is more sensitive to the field.

Some IPBS signatures described in this paper are probably present in published observations. If one compares the Tr1 Stokes V profile depicted in our Fig 2 (upper right panel) with those of Lagg et al. (2004) (Figs 4 and 5), the resemblance is striking. More specifically, the IPBS blueshift and the net offset towards negative values both become immediately apparent. Profile asymmetries are also present in their observations. However, it is not possible to assess whether these arise from IPBS or from velocity or magnetic field gradients.

This work has been partially funded by the Spanish Ministerio de Educación y Ciencia through project AYA2001-1649 and by the European Solar Magnetism Network.

## REFERENCES

- Condon, E. U., & Shortley, G. H. 1970, *The theory of atomic spectra* (Cambridge University Press)
- Lagg, A., Woch, J., Krupp, N., & Solanki, S. K. 2004, *A&A*, 414, 1109
- Landi Degl’Innocenti, E. 1978, *A&AS*, 33, 157
- Landi Degl’Innocenti, E. 1992, in *Solar Observations: Techniques and Interpretation*, First Canary Islands Winter School of Astrophysics, ed. F. Sánchez, M. Collados, & M. Vázquez (Cambridge Univ. Press), 71
- Radzig, A. A., & Smirnov, B. M. 1985, *Reference data on Atoms, Molecules and Ions* (Springer, Berlin)
- Rüedi, I., Solanki, S. K., & Livingston, W. C. 1995, *A&A*, 293, 252
- Trujillo Bueno, J., Landi Degl’Innocenti, E., Collados, M., Merenda, L., & Manso Sainz, R. 2002, *Nature*, 415, 403

---

This 2-column preprint was prepared with the AAS L<sup>A</sup>T<sub>E</sub>X macros v5.2.

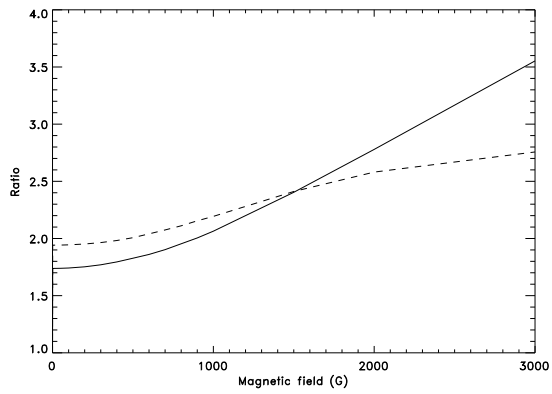


Fig. 6.— Ratio of the Stokes V amplitudes of the red (Tr2+Tr3) and blue (Tr1) components of the multiplet, as a function of the magnetic field for a given model. Solid: IPBS. Dashed: LZS.